night, local time. The heat absorbed by the antenna is transferred through the main bearing assembly to the spinning portion of the spacecraft. Thus, at some time after noon and midnight, the spinning section reaches its maximum temperature, expands to its maximum diameter, and decreases its spin velocity to a minimum. Figure 3 shows maximum spin periods occurring at about 1:00 a.m. and 1:00 p.m., thus indicating a thermal time lag of approximately 1 hr. Telemetry measurements of Westar I solar panel temperatures, taken in early May of 1974, indicate peak-to-peak variations of about 1.1°F. Using this value and the coefficient of thermal expansion of aluminum C, the expected peak-to-peak change in spin period ΔT_s is approximately 19μsec, as shown below in Eqs. (9-11). This estimate compares favorably with the measured peak-to-peak change of 15 μsec.

$$H \simeq M \cdot R^2 . \omega \simeq 2\pi M R^2 / T_s = \text{constant} \tag{9}$$

$$R^2/T_s = (R + C \cdot \Delta T \cdot R)^2 / (T_s + \Delta T_s) \tag{10}$$

$$\Delta T_s \simeq 2C \cdot \Delta T \cdot T_s \simeq 2 \times 13.3 \times 10^{-6} \times 1.1 \times 0.636 \simeq 19 (\mu\text{sec}) \tag{11}$$

where H is angular momentum, R is radius, M is mass, and ω is angular velocity.

Conclusions

The results obtained from the experiment give some indication that the 15μ Earth horizon may be usable as a reference for ultra stable attitude control systems. Conclusive evidence would require an experiment that used 1) a sensor designed for low sample noise and good temperature stability, 2) on-board thresholding circuits that eliminate link noise, interference periods, and ground station uncertainties. Continuous data runs for longer duration could then be obtained to enable more accurate regressions and power density spectrums to be made. An additional result of interest is the semidiurnal spin speed variation caused by the thermal expansion and contraction of the spacecraft.

Noninteger Transfer Orbits for Circular Orbit Phasing Maneuvers

Gordon L. Collyer*
U.S. Army Missile Research and Development Command, Huntsville, Ala.

Nomenclature

a = semimajor axis of an elliptical orbit, ft
e = eccentricity
f = true anomaly, radians
ℓ = parameter in the polar expression for an elliptical orbit, corresponds to the radius for a true anomaly of 90°, ft
P = orbital period, sec
N = integer number of intersatellite transfer ellipses
r = radius, ft
t = transfer duration, sec
V = velocity, fps
ΔV = change in velocity, fps
λ = phase change in circular orbit, radians
θ = apsidal rotation angle, radians
μ = Earth's gravitational constant, ft^3/sec^2

Subscripts

c = circular
E = elliptical
n = nth integer transfer ellipse
R = rotation
1 = first
2 = second

Received April 5, 1976; revision received May 24, 1976.
Index categories: Earth-Orbital Trajectories; Spacecraft Mission Studies and Economics.
*Aerospace Engineer.

Introduction

A DERIVATION for optimal intersatellite transfers between locations in a given circular orbit, subject to a time limitation, is contained in Ref. 1. The transfer technique contained in that analysis involved the familiar method of using an integer number of elliptical phasing orbits, resulting in transfer opportunities only at particular times. The restriction to a discrete transfer scheme is not necessary, however, because of dynamic considerations.

A transfer technique will be developed utilizing, in general, nonintegral transfer ellipses, thereby permitting transfer opportunities as a continuous function of time. As an application, the ΔV for a simple transfer geometry will be analyzed using both the discrete and continuous methods to demonstrate an improved local minimum resulting from the continuous technique.

Transfer Technique

The transfer method presented here employs one or more elliptical transfer orbits with a burn to rotate the line of apsides provided as an additional phasing maneuver. Figure 1 depicts the transfer geometry. Note that three burns are required; the first and last burns comprising the standard Hohmann maneuver. Because the amount of apsidal rotation required becomes a function of the difference between the transfer time and the time corresponding to the last integer revolution opportunity, the geometry reduces to the discrete scheme for times corresponding to these opportunities.

First, an expression for the ΔV required by the rotation burn given the transfer time and the phase change (angular separation), will be developed. The time corresponding to the last integer revolution transfer opportunity is given from

$$t_N = P_c (N - \lambda/2\pi) \tag{1}$$

where N is the associated number of revolutions. For a transfer of specified duration the rotation of the apsidal line necessary for correct phasing becomes

$$\theta = (t - t_N) \frac{2\pi}{P_c} = 2\pi \left[\frac{t}{P_c} - \left(N - \frac{\lambda}{2\pi} \right) \right] \tag{2}$$

Given that only rotation of the apsides is desired, the true anomaly where this rotation is permitted can be found by equating the polar expressions for the orbital radii. The intersection of the orbits is as follows

$$r_1 = r_2 = \frac{\ell}{1 + e \cos(f_1)} = \frac{\ell}{1 + e \cos(f_2)} \tag{3}$$

Since the rotation about the focus is being measured,

$$f_2 = f_1 - \theta \tag{4}$$

Substituting Eq. (4) into Eq. (3) and simplifying

$$\cos(f_1) = \cos(f_1)\cos(\theta) + \sin(f_1)\sin(\theta) \tag{5a}$$

$$\tan(f_1) = \frac{1-\cos(\theta)}{\sin(\theta)} = \tan\left(\frac{\theta}{2}\right) \tag{5b}$$

which is satisfied for f_1 such that $f_1 = \theta/2 + K\pi$, where $K = 0,1,2,3,\ldots$ For $K = 0$, the following is observed

$$f_1 = -f_2 = \frac{\theta}{2} \tag{6}$$

Thus, the rotation ΔV is a pure rotation of the velocity vector at intersection in Fig. 2, given by

$$\Delta V_R = 2\left|e\left(\frac{\mu}{\ell}\right)^{1/2}\sin(f_1)\right|$$

$$= 2\left|e\left(\frac{\mu}{\ell}\right)^{1/2}\sin\left(\pi\left[\frac{t}{P_c} - \left(N - \frac{\lambda}{2\pi}\right)\right]\right)\right| \tag{7}$$

The problem of properly sizing the orbit for a given transfer time remains. From Ref. 2, the flight time required to go from perigee to a particular true anomaly is

$$t(f) = \frac{a^{3/2}}{\sqrt{\mu}}\left[2\tan^{-1}\left(\left[\frac{1-e}{1+e}\right]^{1/2}\tan\left(\frac{f}{2}\right)\right) - \frac{e[1-e^2]^{1/2}\sin(f)}{1+e\cos(f)}\right] \tag{8}$$

Examination of Fig. 1 reveals the following expression for total transfer time (duration)

$$t = N\cdot P_E + 2\cdot t(f_R) = N\cdot\left(\frac{2\pi\, a^{3/2}}{\sqrt{\mu}}\right) + 2\cdot t(f_R) \tag{9}$$

For N greater than or equal to 1, N revolutions would be made in the nonrotated orbit, initiated by burn A, the first Hohmann burn. During the last orbit, burn B would be made at the proper true anomaly to rotate the orbit. Note that angular travel during the last orbit would be greater than or equal to 2π. Burn C, the second Hohmann burn, would complete the transfer sequence at rendezvous.

Substituting Eqs. (6) and (8) into Eq. (9) yields the following transcendental relationship between the transfer time desired and the semimajor axis of the transfer ellipse

$$t = \frac{2\, a^{3/2}}{\sqrt{\mu}}\left[N\cdot\pi + \left(2\cdot\tan^{-1}\left[\left[\frac{1-e}{1+e}\right]^{1/2}\tan\left(\frac{\theta}{4}\right)\right] - \frac{e[1-e^2]^{1/2}\sin\frac{\theta}{2}}{1+e\cos\frac{\theta}{2}}\right)\right] \tag{10}$$

It is noted that from Eq. (2), θ is a function of the transfer time (λ and N specified); and that the eccentricity e, as a function of the semimajor axis for an ellipse with perigee or apogee at circular radius (R_c), can be expressed as

$$e = |R_c/a - 1| \tag{11}$$

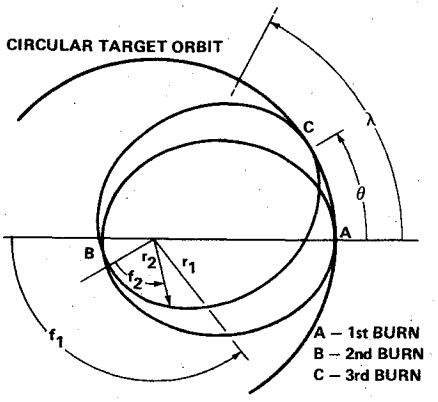

Fig. 1 Transfer geometry.

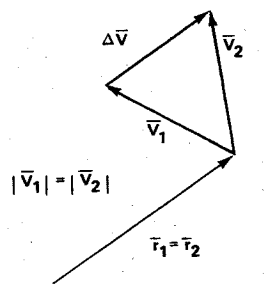

Fig. 2 ΔV for pure rotation.

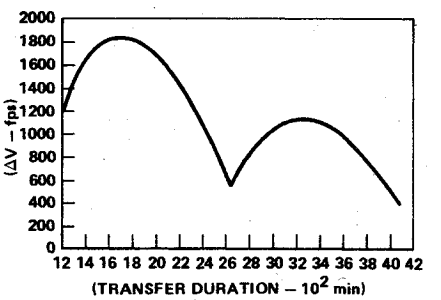

Fig. 3 Total ΔV for transfer ($\lambda = 55°$).

The ΔV required for a specified transfer time is found by first sizing the transfer orbit with the determination of the semimajor axis that satisfies Eq. (10). The rotation ΔV required is determined from Eq. (7) and added to the Hohmann ΔV required for burning in and out of the transfer ellipse to give the total energy requirement for the maneuver. Figure 3 is the total ΔV as a function of transfer duration for an intersatellite transfer of 55° in circular synchronous equatorial orbit using the time continuous transfer technique previously developed.

Table 1 Results for optimal discrete transfers

λ (deg)	t (min)	Number of revolutions	ΔV (fps)
55	2652.7	2	556.5
150	2273.8	2	1778.4
205	4926.5	4	2334.9

Table 2 Results using the nonliner transfer scheme

λ (deg)	t (min)	Number of revolutions	ΔV (fps)
55	2509.1	1.9	889.2
150	3709.8	3.0	1086.7
205	6218.9	4.9	1975.9

Comparison to Optimal Discrete Transfers

Consider a mission sequence in circular synchronous equatorial orbit consisting of two transfers of 55 and 150° each. In addition, a time limitation of 6219 min. is imposed. The optimal distribution of integer phasing ellipses using the method of Ref. 1 is shown in Table 1.

Note that the total of 4 integer revolutions is the maximum possible, for the time limit assumed, using the discrete method. Using the continuous technique, which allows fractional revolutions for the 55-degree transfer, the distribution of Table 2 is found. Using a continuous transfer scheme has, for this example, reduced the ΔV requirement by 15.4%.

References

[1]Fallin, E. H., III, "Optimal Intersatellite Transfers for On-Orbit Servicing Missions," *Journal of Spacecraft and Rockets*, Vol. 12, Sept. 1975, pp. 565-568.

[2]Thomson, William T., *Introduction to Space Dynamics*, Wiley, New York, 1961.

Lightweight, Low-Cost EVA Range Estimation Aid

Wallace T. Fowler*
University of Texas at Austin, Austin, Texas
and
David B. Higginst
SAMCO, Los Angeles, Calif.

ONCE the space shuttle becomes operational, extravehicular activities (EVA) by astronauts not physically attached to the shuttle will become commonplace. The EVA astronauts will use manned maneuvering unit (MMU) for propulsion, and can be expected to range at least as far as 500 m from the shuttle on early missions. The MMU will most likely be equipped with a lightweight radar unit for use as the primary means of range and range rate determination. The possibility exists to provide the astronaut with a backup range finder at extremely low cost. The Note discusses such a backup range finder.

At first glance, it seems that since the astronaut "knows" the size of the shuttle, he should be able to estimate the range between himself and the shuttle with no equipment at all should his radar fail. Researchers in the psychophysics of vision, such as Galanter and Galanter,[1] seem to feel that with training, a person can estimate range and range rate with reasonable accuracy. However, most of the research in this area has been limited to familiar targets in a visual field abundant with nearby referents. Very little has been done in a visual field consisting solely of a familiar object at close range.

Since we are unsure of the range estimation abilities of an astronaut in the space environment, and since the consequences of an erroneous range estimate could be serious, an MMU manual rangefinder has been devised. This rangefinder is simple, lightweight, cheap, and has no moving parts. It is designed to give the astronaut a rapid rough estimate of his distance from the shuttle (a similar rangefinder could be developed for any object of known size and shape).

Received April 23, 1976.
Index categories: Extra-Vehicular Activity; Data Sensing and Presentation or Transmission System.

*Associate Professor, Department of Aerospace Engineering and Engineering Mechanics. Member AIAA.
†2nd Lieutenant, USAF. Member AIAA.

The rangefinder is based on the well-known principle that the angle subtended by an object of known size is a function of its orientation and its distance from the observer. A brief review of the physical principle will now be given. Let d be some known readily observable physical dimension of the object to which range is being measured. For example, d might be the length, span, height, fuselage thickness, or vertical stabilizer leading-edge length of the shuttle. Although the astronaut might have scales for each of these, for the presentation here we will consider only one such observable physical dimension. Let us, for example, choose the span of the shuttle as the physical dimension upon which our range measurement might be based.

Thus, for the example $d=S_s$, where S_s is the span of the shuttle. For simplicity, let us first assume that the astronaut is directly behind the shuttle, (in the shuttle fixed $y\,z$ plane). The shuttle is assumed to be oriented so that it is flying like an airplane down the flight path (wings level, upright, nose forward).

The device works in the following manner: The astronaut "holds" a graduated scale at arms length perpendicular to the line of sight between his eye (one eye closed) and the shuttle. The scale is held so that its graduated length lies in a plane parallel to the lateral axis of the shuttle. The edge of the scale is held so that the astronaut can read the number of scale graduations subtending the same angle which is subtended by the span of the shuttle. He reads the number of graduations and then looks to a distance scale which is calibrated on shuttle span for the range to the shuttle.

At large distances $s_s \cong r\theta$. Also $\ell_s \cong a\theta$ (see Fig. 1). For any given astronaut, a is a fixed quantity, i.e., arms length. The scale could be individualized so that a given range r the shuttle subtends the same number of scale divisions, regardless of the astronaut.

From the two approximate relations, the angle θ can be eliminated to give

$$\frac{\ell_s}{L_s} = \frac{a}{r} \quad \text{or} \quad r = \frac{L_s}{\ell_s} a$$

In order to place this information in a format easily usable by the astronaut, a scale such as that shown in Fig. 2 is provided. If, for example, the span of the shuttle subtends ten graduations, as shown, then the astronaut is about 190 to 200 m from the shuttle.

Several scales such as that shown in Fig. 2 (for length, span, fin height, etc.) would suffice if we could insure that the astronaut would always be in a position to view the shuttle so that the dimension being used as a reference is perpendicular to the line of sight. This is obviously not the case. Thus, we must provide the astronaut with some method of correcting for the visual foreshortening of the reference length when

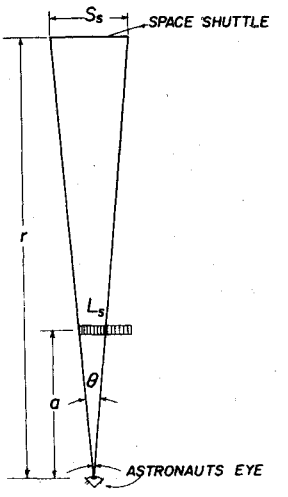

Fig. 1 Range finder geometry.